Evaluation of the Flow-Dialysis Technique for Analysis of Protein-Ligand Interactions: An Experimental and a Monte Carlo Study

Gertjan Veldhuis, Erwin P. P. Vos, Jaap Broos, Bert Poolman, and Ruud M. Scheek
Department of Biochemistry and Biophysical Chemistry, Groningen Biomolecular Science and Biotechnology Institute, University of Groningen, 9747 AG Groningen, The Netherlands

ABSTRACT Flow dialysis has found widespread use in determining the dissociation constant (K_D) of a protein-ligand interaction or the amount of available binding sites (E_0). This method has the potency to measure both these parameters in a single experiment and in this article a method to measure simultaneously the K_D and E_0 is presented, together with an extensive error analysis of the method. The flow-dialysis technique is experimentally simple to perform. However, a number of practical aspects of this method can have a large impact on the outcome of K_D and E_0. We have investigated all sources of significant systematic and random errors, using the interaction between mannitol and its transporter from *Escherichia coli* as a model. Monte Carlo simulations were found to be an excellent tool to assess the impact of these errors on the binding parameters and to define the experimental conditions that allow their most accurate estimation.

INTRODUCTION

The strength and stoichiometry of protein-ligand interactions are important parameters for understanding the biological properties of proteins. The strength of the protein-ligand interaction, usually expressed as the dissociation constant K_D, is a measure for the free energy associated with this interaction. Understanding of the protein-ligand interaction at the molecular level can be obtained by investigating the impact of changes in buffer composition, pH, or temperature, or by studying the effects of changes in substrate structure or mutations in the protein on the interaction. Investigations of allosteric mechanisms, enzyme inhibition, or competitive ligand interactions all rely on accurate estimation of both the dissociation constant (K_D) and the stoichiometry of this interaction, the number of binding sites present (E_0).

A number of experimental approaches is available to study protein-ligand interactions. When the protein and the ligand have sufficiently different sizes, various separation techniques, e.g., size-exclusion chromatography or equilibrium dialysis, can be employed to measure separately the concentrations of bound and unbound ligand. In equilibrium dialysis, the actual concentrations of interacting species are measured after equilibrium has been established between two compartments separated by a semipermeable membrane. This is a relatively slow technique, making this approach less suitable when one of the components is labile, or for high-throughput screening programs.

The actual chemical equilibrium between ligand and protein is usually reached within minutes or seconds. This led Colowick and Womack to develop a rapid method for measuring binding of ligand molecules that are able to diffuse across a semipermeable membrane: the flow-dialysis technique (Colowick and Womack, 1969; Womack and Colowick, 1973). The system consists of an upper chamber containing the protein-ligand system under investigation, and a lower chamber, separated from the upper chamber via a semipermeable dialysis membrane, through which a mobile phase flows. At a given flow rate, the concentration of ligand measured in the mobile phase is proportional to the concentration of free ligand in the upper chamber. This technique has found widespread use ever since (André and Linse; 2002; England and Hervé, 1992; Hellingwerf and Konings, 1980; Lolkema et al., 1990, 1992; Lolkema and Robillard, 1990; Porumb, 1994; Westerhoff et al., 1989).

Usually, a relatively small amount of radioactive ligand is added to a large pool of potential binding sites at protein concentrations that cause practically all ligand to be bound. By adding unlabeled ligand, the bound labeled ligand is replaced with the unlabeled ligand and appears in the mobile phase. At the end, an excess of unlabeled ligand is added to chase all labeled ligand from the binding sites. The radioactivity measured in the mobile phase then corresponds to all the radioactive ligand being unbound, as in an experiment without protein. Evaluation of the concentration of the labeled ligand in the mobile phase during such a titration yields the binding parameters (K_D and E_0).

In this article we present a different approach to obtain K_D and E_0 using flow dialysis. Cumulative amounts of radioactively labeled ligand are added to a fixed amount of binding sites in the regime of ligand concentrations from below the dissociation constant to near saturation. This approach enabled us to accurately determine both the K_D and E_0 with one sample in a single experiment within ~30 min.

Several reports in the literature have indicated that improper analysis of the obtained data (e.g., ignoring background signal, overlooking nonspecific binding, a nonlinear relationship between a measured signal and the

Submitted September 16, 2003, and accepted for publication December 4, 2003.

Address reprint requests to Ruud M. Scheek, Tel.: +31-50-3634328; Fax: +31-50-3634800; E-mail: scheek@chem.rug.nl.

Abbreviations used: CPM, counts per minute; dPEG, decylpoly(ethylene glycol) 300; EII^{mtl}, enzyme II^{mtl} from *Escherichia coli*; ISO, inside-out; *LR*, leak rate; MC, Monte Carlo; mtl, mannitol.

0006-3495/04/04/1959/10 $2.00

concentration of bound or free ligand, or the presence of partially inactivated components) and the use of inappropriate mathematical procedures to evaluate the data can cause severe bias in the obtained ligand binding parameters (Fuchs and Gessner, 2001; Larsson, 1997; Rovati et al., 1988; Schumacher and Von Tscharner, 1994). Thus, although flow dialysis is experimentally a simple and fast technique, accurate determination of the protein-ligand parameters necessitates a thorough evaluation of the experimental procedure. The use of a semipermeable membrane necessarily entails a certain leak of the labeled ligand (typically 0.5–1.0%/min). Preliminary work in our group indicated that leakage of ligand at such rates during a flow dialysis experiment has a significant impact on the apparent binding parameters, so this effect has to be properly corrected for. An extensive error analysis of the flow-dialysis experiment is presented, including Monte Carlo simulations to evaluate the effects of the relevant systematic and nonsystematic errors, and to define the experimental conditions that allow accurate estimation of the important binding parameters.

EXPERIMENTAL METHODS

Chemicals

D-[1-^{3}H(N)]Mannitol (17.0 Ci/mmol) was purchased from NEN Research Products (Boston, MA). D-[1-^{14}C]Mannitol (59.0 mCi/mmol) was purchased from Amersham Biosciences (Uppsala, Sweden). Radioactivity measurements were performed using Emulsifier Scintillator Plus obtained from Packard (Groningen, The Netherlands). dPEG was obtained from Kwant High Vacuum Oil Recycling and Synthesis (Bedum, The Netherlands).

Cell growth and isolation of ISO membrane vesicles

Plasmids harboring the wild-type *mtlA* gene or the mutant *mtlA-G196D* gene were transformed and subsequently grown in bacterial strain *Escherichia coli* LGS322 as described (Boer et al., 1995). LGS322, not transformed, and thus not expressing the *mtlA* gene, was used in control experiments (LGS^{minus}). ISO membrane vesicles were prepared essentially as described (Broos et al., 1999). The vesicles were washed once with 25 mM Tris-HCl, pH 7.6, 1 mM dithiotreitol, and 1 mM NaN_3, and quickly frozen in small aliquots in liquid nitrogen for storage at −80°C. Vesicles used for experiments were placed at 37°C for quick thawing and directly placed on ice until further use.

The flow dialysis system

The system as described by Lolkema et al. (1990) was used and a schematic representation is shown in Fig. 1. It consists of a dialysis cell with a 1.2 mL cylindrical upper compartment containing the enzyme solution. It is separated by a dialysis membrane (ServaPor, SERVA Electrophoresis, Heidelberg, Germany), molecular mass cutoff 14,000 Da) from the lower part: a spiral groove with a volume of 20 ± 1 μL engraved in a solid support (Feldmann, 1978).

The mobile phase has a flow rate of 230 μL/min and is connected to a fraction collector via 30 cm tubing with an inner diameter of 0.5 mm, corresponding with 60 μL. A Teflon-coated magnetic bar (7 × 2 mm) stirs the upper compartment. The whole system was thermostated at 25 ± 0.1°C. All experiments were performed in 25 mM Tris-HCl, pH 7.6, 5 mM dithiotreitol, and 5 mM $MgCl_2$ with 0.25% dPEG, unless stated otherwise. The upper compartment usually contained between 50 nM and 25 μM of binding sites, in 300–500 μL of the above buffer solution. The experiment was started after the protein solution had been equilibrated for 10 min at 25°C.

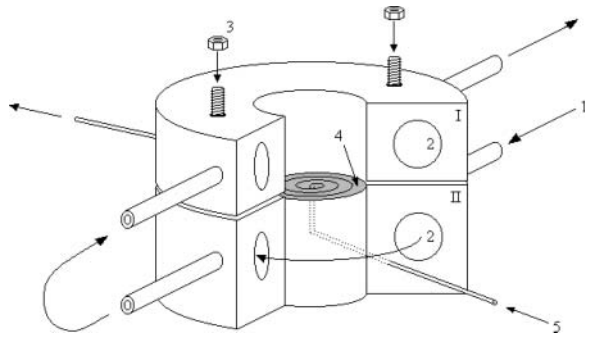

FIGURE 1 Schematic representation of the flow dialysis cell. (*1*) Inlet of water from water bath at specific temperature. (*2*) Channels through the system for thermostatic use. (*3*) Upper part is fastened to the lower part to seal the contents of the lower spiral groove from the upper sample chamber. (*4*) The dialysis membrane (*shaded*) is stretched over the spiral groove and extends somewhat between the two domes. (*5*) Inlet of flow-through buffer (mobile phase) reaches the membrane in the middle and follows the spiral groove to the exit.

A typical flow dialysis experiment

A control experiment is carried out to estimate the rate of diffusion of the labeled ligand across the membrane (the leak rate) and the dead time of the system. In the control experiment, the upper compartment is filled with buffer solution and samples are collected for 20 min after the flow is started. After the first sample (six droplets) is collected, a known concentration of radioactive ligand (25–100% of the total concentration used in the experiment with protein) is introduced in the upper compartment. Sampling is continued during the next 9–10 min, after which a second addition of the same amount of radioactive ligand is made. The radioactivity of the collected samples was measured after addition of 2.0 mL of scintillation fluid. The background radioactivity (as determined from the first collected sample) was subtracted from all samples. A plot of the CPMs in the collected samples against the time yields two values for the leak rate (*LR*, %/min), and two values for the multiplication factor β, relating measured radioactivity and concentration of free ligand in the upper compartment. These values are averaged and used as such.

For each flow-dialysis experiment, a new dialysis membrane was used. The titration experiment with protein consists of 9 or 10 cycles of addition of radioactive ligand, equilibration, and sampling, each cycle taking exactly 3 min. The experiment is started by mixing all components and applying the sample with protein to the upper chamber. At $t = 0'$, a certain amount of radioactive ligand is applied to the upper chamber; 1 min after the addition of radioactive ligand, when the binding equilibrium already has been reached (Lolkema et al., 1990), the radioactivity in the mobile phase is measured by collecting, during 1.5 min, five samples of six droplets each for radioactivity counting. This cycle is repeated 9–10 times. Fig. 2 shows the precise time schedule employed during the titration cycles.

Theoretical background

Table 1 shows a glossary of symbols and definitions used in this article. For the equilibrium between a single ligand-binding, noncooperative enzyme (*E*) with ligand (*S*),

$$E + S \Leftrightarrow ES, \tag{1}$$

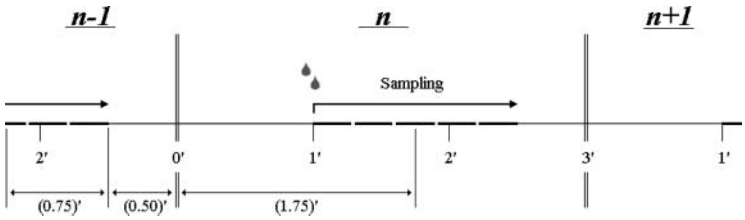

FIGURE 2 Schematic representation of the time regime for leak (ΔS_{leak}) determination. Relevant equation (Eq. 5): $\Delta S^{n}_{leak} = 1.25 \times LR \times S^{n-1}_{free} + 1.75 \times LR \times S^{n}_{free}$. The leak at each point n consists of two components. The first component (1.25′, in minutes) is the leak from the previous addition ($n - 1$) from halfway sampling until the end of sampling (0.75′) plus the remaining time until the next addition at point n (0.50′). The second component starts from the point of addition of a new amount of substrate at point n and lasts until halfway the sampling during n (1.75′).

the concentration of unbound ligand (S_{free}) as a function of the total ligand (S_{tot}) and total protein (E_{tot}) concentrations can be written as follows:

$$S_{free} = 0.5 \times \left(S_{tot} - E_{tot} - K_D + \sqrt{(S_{tot} - E_{tot} - K_D)^2 + 4 \times S_{tot} \times K_D}\right), \quad (2)$$

with the equilibrium constant K_D defined as:

$$K_D = \frac{E \times S}{ES}. \quad (3)$$

In the upper compartment containing the protein, the total amount of ligand present at each cycle n (S^{n}_{tot}) is given by

$$S^{n}_{tot} = S_0 \times \frac{\sum_{i=1}^{n} \Delta V^{i}}{V_0 + \sum_{i=1}^{n} \Delta V^{i}} - \sum_{i=1}^{n} \left|\Delta S^{i}_{leak}\right|, \quad (4)$$

in which ΔV^i is the volume of added ligand at step i, V_0 the initial volume in the upper compartment, and S_0 the concentration of ligand in the stock solution. ΔS^{i}_{leak} is the drop in the ligand concentration due to leak through the membrane at step i. In our system, the leak rate LR is small (usually <1%/min) and therefore the leak can be treated as a zero-order process. This makes it legitimate to average the five fractions during the same cycle. The time between halfway the sample collection of the previous titration cycle ($n - 1$) and halfway the sampling of cycle n is used to calculate the leak correction for cycle n. In our titration schedule (Fig. 2), these points are 1.25 min before and 1.75 min after the start point of cycle n, respectively, resulting in the following expression for the drop in the total ligand concentration due to leakage:

$$\Delta S^{n}_{leak} = 1.25 \times LR \cdot S^{n-1}_{free} + 1.75 \times LR \times S^{n}_{free}. \quad (5)$$

The total protein concentration at each point n (E^{n}_{tot}) is only dependent on the dilution caused by the addition of S, according to:

$$E^{n}_{tot} = E_0 \times \frac{V_0}{V_0 + \sum_{i=1}^{n} \Delta V^{i}}. \quad (6)$$

Equations 2, 4, and 6 then yield a value for S^{n}_{free} at each titration point. Multiplying S^{n}_{free} with β gives the signal C^n (CPMs measured after n additions):

$$C^{n} = \beta \times S_{free} = 0.5 \times \beta \times \left(S_{tot} - E_{tot} - K_D + \sqrt{(S_{tot} - E_{tot} - K_D)^2 + 4 \times S_{tot} \times K_D}\right). \quad (7)$$

Summarizing the procedure thus far, the raw data (i.e., total added volume $\left(\sum_{i=1}^{n} \Delta V^{i}\right)$ from the ligand stock solution and the radioactivity counted in the mobile phase at each titration step n) are used to calculate (Eqs. 4 and 5) the total ligand concentration S^{n}_{tot} (corrected for the ongoing leak through the semipermeable membrane) and the concentration of free ligand (S^{n}_{free}). For this we use the values for β and the leak rate obtained from the control experiment. This leaves only the values of K_D and E_0 (and sometimes β, see below) to be determined by fitting the experimental data (C^n) to Eq. 7. For this, any mathematical software package able to perform nonlinear least-squares minimization can be used. We chose the Levenberg-Marquardt algorithm.

However, since weight factors cannot be assumed to be the same for each titration point, they have to be calculated separately for each titration point, as will be shown below. Also, because the number of titration points is not enough to estimate the confidence intervals for the fitting parameters from the spread in the experimental values, we chose to implement a Monte Carlo approach to this end. All routines used were written in the software package Mathematica 4.1 (available on request).

The error function that has to be minimized is defined as:

$$\chi^2 = \sum_{n=1}^{N} w^{n} \times \left(C^{n} - C^{n}_{calc}\right)^2, \quad (8)$$

with the weight w^n of each data point taken as the inverse of the variance of the signal measured during cycle n:

$$w^{n} = \frac{1}{\sigma^2_{C^n}}. \quad (9)$$

TABLE 1 Glossary of symbols and definitions

Symbol	Definition
V_0	Initial volume of protein solution in the flow chamber
ΔV^i	Volume added at addition i
σ^i	Standard error in ΔV^i
S_0	Ligand concentration in stock solution
E_0	Initial concentration of binding sites in upper compartment
S^{i}_{tot}	Total concentration of ligand at titration point i
E^{i}_{tot}	Total concentration of binding sites at titration point i
ΔS^{i}_{leak}	Correction for leak of ligand at sampling point i
C^i	Signal measured in samples after addition i
C^{i}_{calc}	Calculated signal after addition i
K_D	Dissociation constant
LR	Leak rate (%/min)
β	Ratio between CPM and free ligand concentration
w^i	Weight of data point i

The variance in the signal measured during cycle n is calculated as follows. The standard deviation in the total ligand concentration after n additions ($\sigma_{S_{tot}^n}$) is dominated by the accumulated errors in the added volumes ΔV^i:

$$\sigma_{S_{tot}^n} = \sqrt{\sum_{i=1}^{n} (\sigma^i)^2} \times \frac{S_0}{V_0 + \sum_{i=1}^{n} \Delta V^i}. \quad (10)$$

The absolute error ($\sigma^i = 0.04\ \mu L$) in pipetting was determined experimentally by weighing. Equation 10 yields the standard deviation of the total ligand concentration. Variations in the ligand concentration directly influence the signal C. Therefore, the first derivative of the signal C with respect to the total ligand concentration (Eq. 7) is used to evaluate the effect of variations in the total ligand concentration on the signal C^n:

$$\sigma_{C^n}^{\Phi 1} = \left| \left(\frac{\partial C}{\partial S_{tot}} \right)_{S_{tot}=S_{tot}^n} \right| \times \sigma_{S_{tot}^n}. \quad (11)$$

This derivative is calculated numerically by incrementing S_{tot} with a very small amount and calculating the quotient $\Delta C^n/\Delta S_{tot}$.

The standard deviation in the signal due to counting uncertainties is given by:

$$\sigma_{C^n}^{\Phi 2} = \sqrt{\frac{C^n}{5}}. \quad (12)$$

The factor 5 arises from the averaging of the five samples collected per cycle. Being independent, these two contributions to the standard deviation in the measured signal C^ncan be squared and summed to yield the total variance (σ^2):

$$\sigma_{C^n}^2 = \left(\sigma_{C^n}^{\Phi 1}\right)^2 + \left(\sigma_{C^n}^{\Phi 2}\right)^2, \quad (13)$$

which is used to determine the weight of each data point according to Eq. 9.

The impact of each error source on both the K_D and E_0 can be investigated by a MC simulation, offering the possibility to optimize an experimental setup. The Monte Carlo computer simulations generate many virtual data sets as follows. For each addition, a value for ΔV^i is taken at random from a normal distribution around the actual value used in the experiment, with a standard deviation equal to σ^i (e.g., 0.04 μL). Equations 4–7 are then used to calculate the corresponding signal. For the parameters LR and β, the experimental values are taken as such. For the parameters K_D and E_0, the values are used that yielded the best fit of Eq. 7 to the real experimental data. The counting error in the calculated signal is incorporated by replacing the calculated value for C^n by a value taken at random from a normal distribution around C^n with a standard deviation equal to $\sqrt{C^n}$. This approximates the expected Poisson distribution very well. These virtual data sets are subsequently analyzed exactly as the real experimental data sets, and the observed variation in the best-fit parameters is taken to be an accurate representation of the real variation to be expected in experimentally obtained binding parameters. Apart from the nonsystematic errors mentioned, also the effects of systematic errors (use of incorrect weights for the data points, incorrect choice of the parameters LR or β) could be investigated with these virtual data sets, as will be shown below.

RESULTS

The enzyme we used to evaluate the method is the mannitol transporter from *E. coli*, EII^{mtl}. It resides in the inner membrane and exhibits high-affinity mannitol binding in the nanomolar regime. Mutating the enzyme, by replacing glycine 196 for an aspartate (EII-G196D), results in mannitol binding with an affinity in the micromolar regime (Boer et al., 1995). For both enzymes, flow dialysis experiments are presented, including the control experiments, the fitting procedure, the impact of ligand leak on the apparent binding parameters (K_D and E_0), and the calculation of weight factors for the individual data points. The confidence limits of the binding parameters are determined by Monte Carlo computer simulations, taking the most important random errors into account.

High-affinity mannitol binding

Fig. 3 shows the results of a binding experiment, executed as described in the Experimental Methods section, using wild-type EII^{mtl} and [^{3}H]mannitol. From the control experiment

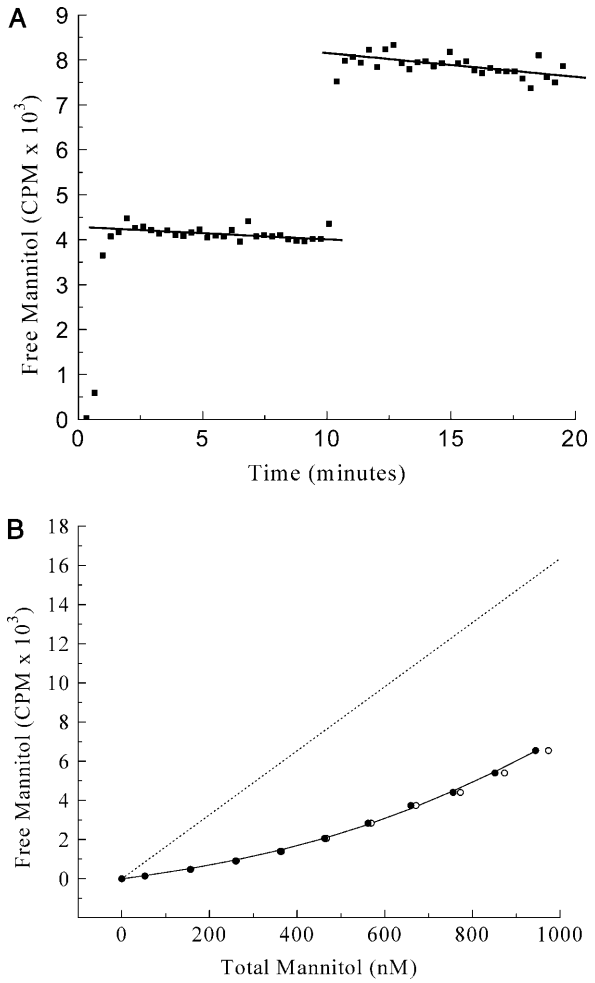

FIGURE 3 High-affinity mannitol binding to wild-type EII^{mtl}. (*A*) Control experiment. Two additions, each 5 μL of 20.0 μM [^{3}H]mannitol to 380 μL buffer in the dialysis cell. Solid lines represent linear fits. (*B*) Mannitol titration curve with additions of 1 × 1.0 μL and 9 × 2.0 μL of 20.0 μM [^{3}H]mannitol. Dotted line was drawn using the β-value obtained from Fig. 3 *A*. (○) Uncorrected data; (●) data points corrected for leakage (see text).

(Fig. 3 *A*), a value of 0.63%/min was calculated for the *LR* and a value of 16.34 CPM/nM for the factor β, which relates the radioactivity measured in the mobile phase with the concentration of unbound mannitol in the upper compartment.

ISO *E. coli* membrane vesicles, containing an amplified level of EII^{mtl}, were used as the source of EII^{mtl} for the titration shown in Fig. 3 *B* at a total membrane protein concentration of ~1 mg/mL. The buffer used included the detergent dPEG, which efficiently solubilizes the vesicles, thus preventing any buildup of mannitol inside the vesicles and making all binding sites available. The enzyme was stable under these conditions, and solubilization by dPEG only marginally affected the binding characteristics (Lolkema et al., 1993). Fitting of these data using Eq. 7, not corrected for mannitol leakage (*open circles* in Fig. 3 *B*), yielded a K_D of 205 nM and an E_0 of 909 nM.

The correction for mannitol leakage has a significant effect on the binding parameters. Values for K_D and E_0 of 179 nM and 828 nM, respectively, were obtained when a leak rate of 0.63%/min was used in Eq. 5 for the leak correction (*solid circles* in Fig. 3 *B*).

The use of proper weight factors for the individual data points further improved the reliability of the obtained parameters. First the data were fitted with equal weights for each point. The best-fit values for the fitting parameters K_D and E_0 were then used to calculate improved weights (Eqs. 9–13) and improved values for K_D and E_0. This process was repeated until stable values for K_D and E_0 were obtained, resulting in a K_D of 155 ± 23 nM and an E_0 of 780 ± 46 nM, respectively (see Fig. 3 *B*, *solid circles*, *connected*). The weight factors employed varied from 5.4×10^{-3} for the first to 3.9×10^{-5} for the last titration point, emphasizing their importance for a correct analysis.

Low-affinity mannitol binding

Low-affinity mannitol binding was investigated with mutant EII-G196D. This mutant shows mannitol binding affinity in the micromolar regime (Boer et al., 1995). The control experiment (Fig. 4 *A*) was performed with a 3.39 mM [^{14}C]mannitol stock. From both mannitol leak decays, the *LR* and β-values were determined and averaged. This resulted in an *LR* of 1.03%/min and a β-value of 0.140 CPM/nM.

For the binding experiment with the EII-G196D protein (Fig. 4 *B*), a similar titration scheme as for high affinity binding was used. To vesicles, ~20 mg/ml total membrane protein, 5 mM $MgCl_2$, and 1.0% dPEG were added, and the mixture was incubated at 25°C for 10 min. The 20-fold higher concentration of vesicles used in this experiment had no effect on the leak rate or β-value. This was established by using *E. coli* vesicles not containing EII^{mtl} (LGS^{minus} strain, see Experimental Methods). Fitting of the raw data resulted in a K_D of 88 μM and an E_0 of 95 μM (Fig. 4 *B*, *open circles*). Correction for mannitol leak as described for the high affinity experiments on wild-type EII^{mtl} resulted in a K_D of 37 μM and an E_0 of 52 μM. Complete analysis, including proper weight factors for the data points, resulted in a K_D of 25 ± 6 μM and an E_0 of 46 ± 8 μM (Fig. 4 *B*, *solid circles*). The standard deviations reported in this and the previous section were calculated from the quality of the fit and are not very reliable due to the small number of titration points. A better procedure for estimating the reliability of the binding parameters will be given below.

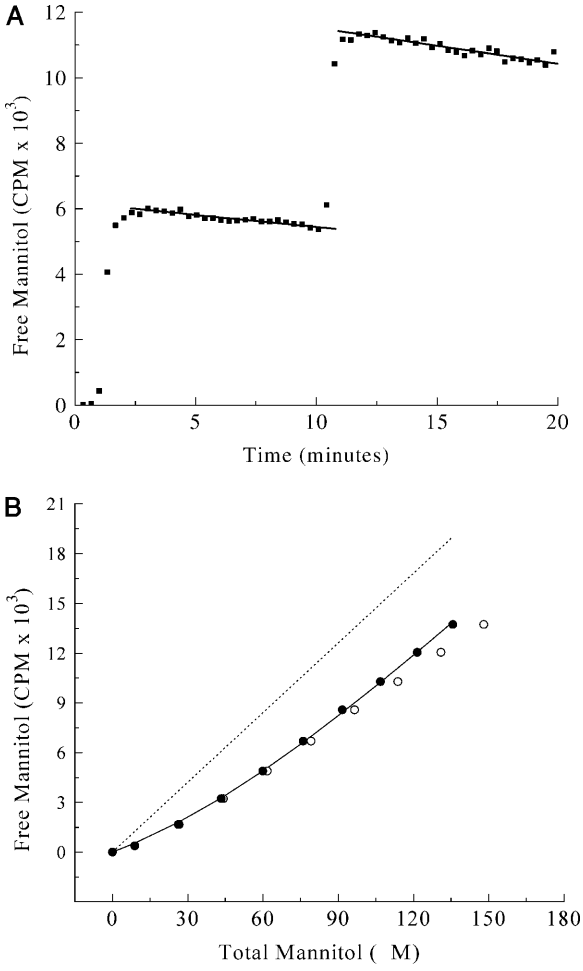

FIGURE 4 Low-affinity mannitol binding to EII-G196D. (*A*) Control experiment. Two additions, each 5 μL of 3.39 mM [^{14}C]mannitol to 380 μL buffer in the dialysis cell. Solid lines represent linear fits. (*B*) Mannitol titration curve with additions of 1 × 1.0 μL and 8 × 2.0 μL of 3.39 mM [^{14}C]mannitol. Dotted line was drawn using the β-value obtained from Fig. 4 *A*. (○) Uncorrected data; (●) data points corrected for leakage (see text).

Monte Carlo simulations

Accuracy of the procedure

For an accurate determination of both the dissociation constant and the number of available binding sites in a single experiment, it is important to choose the amount of protein and the ligand concentration range so that both parameters can be optimally determined. Since the flow-dialysis pro-

cedure relies on the determination of the fraction of the total added ligand that is freely diffusible across the membrane, it is crucial that during a titration a significant fraction of the total added ligand is actually bound. In addition, as in any binding experiment, a high degree of saturation of the binding sites (>80%) must be realized. This leads to the following two important requirements for a good flow-dialysis experiment:

1. The total added ligand concentration must be varied from 0 to n times the total concentration of binding sites, with n in the range of 2–5.
2. The free ligand concentration must vary during a titration from 0 to k times the relevant K_D, with k at least 4 (to reach 80% saturation).

To establish quantitatively how the choice of conditions affects the accuracy of binding experiments, we carried out a large number of Monte Carlo simulations of such experiments. For these calculations we chose $K_D = 1$, and E_0 in the range 1–300. Each simulated titration consists of eight additions of ligand from a stock solution (relative volume increments 1, 2, 2, 2, 2, 4, 4, and 8 μL, with a standard deviation of $\sigma^i = 0.08$ μL) to an initial volume of 380 μL in the upper compartment. The concentration of the stock solution was chosen such that an excess of $n = 3.7$ of total added ligand over the binding sites was reached at the end of the titration. For each addition the total concentrations of ligand and binding sites were calculated (Eqs. 2 and 4), and from these the expected signal (Eq. 7). The β-value was chosen inversely proportional to the concentration of ligand in the stock solution to ensure that in every titration the signal reached similar values. Fig. 5, *A–F*, show some typical (virtual) binding experiments and the resulting distributions of binding parameters obtained from 200 of such virtual data sets, for a range of E_0 values between 1 and 300. Fig. 6 shows the obtained accuracy for both parameters under the different conditions (*solid symbols*: *squares* for the K_D, *circles* for E_0). Clearly, the optimal range for E_0 is between 3 and 30, if both K_D and E_0 need to be determined. Since we did not specify the concentration units in these calculations we can extrapolate this to other values for the K_D by multiplying all concentrations with the actual K_D value of the system under study. So, for our high affinity binding experiments ($K_D = \sim$150 nM), the optimal range for E_0 is

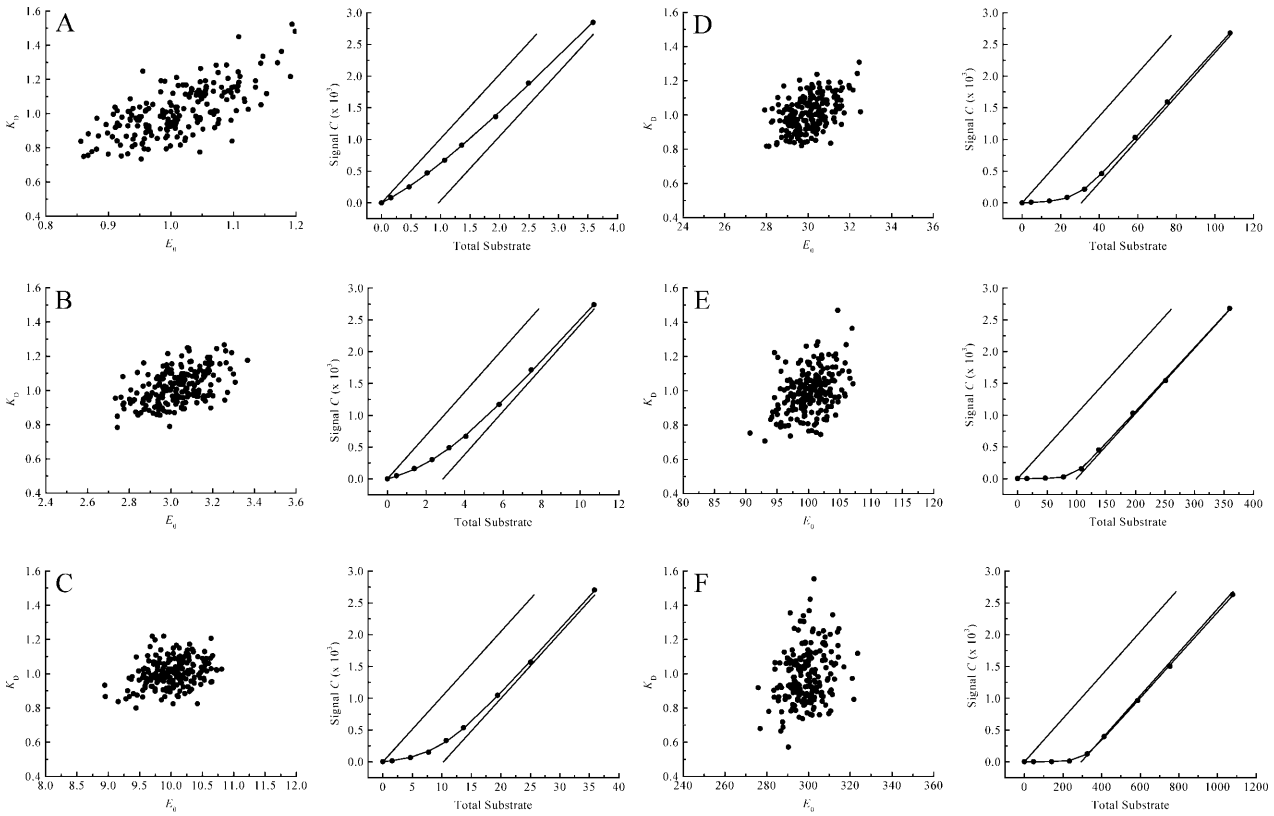

FIGURE 5 Monte Carlo simulations at different E_0/K_D ratios to evaluate the accuracy of the flow dialysis procedure. Each simulated titration consists of eight additions (relative additions: 1, 2, 2, 2, 2, 4, 4, and 8 μL to 380 μL initial volume) of substrate with $\sigma^i = 0.08$ μL. For every E_0/K_D ratio, 200 virtual data sets were generated and fitted. Typical example titration curves of one of the virtual data sets together with the scatter plots are shown (E_0/K_D ratios for *A*, *B*, *C*, *D*, *E*, and *F*, are 1, 3, 10, 30, 100, and 300, respectively). The solid lines in these titration graphs represent the value of β, relating the signal C with the concentration of free ligand. Note that all concentration units are arbitrary and can be scaled at will.

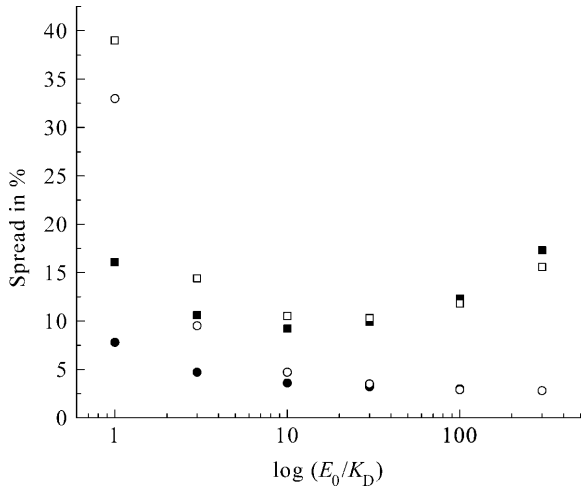

FIGURE 6 Accuracy for both the K_D and E_0 at different conditions. Experimental conditions are as stated in the legend of Fig. 5. Squares represent the spread (%) in K_D, circles the spread in E_0: solid for two-parameter fitting (K_D and E_0), open for three-parameter fitting (K_D, E_0, and β).

between 3 and 30 × 150 nM. For the low-affinity ($K_D = 25$ μM) experiments, the concentration of binding sites should be chosen between 3 and 30 × 25 μM for optimal accuracy.

Nonsystematic errors

To investigate the impact of the pipetting error σ^i, we used values for the K_D and E_0 of 1 and 10, respectively, to generate 200 virtual data sets, as described in the Experimental Methods section, mimicking the conditions and procedures of real binding experiments. Four different values for the pipetting error σ^i were used. These simulated data sets were analyzed exactly as described for the real data, each data set yielding best-fit values for the model parameters K_D and E_0. Table 2 shows the resulting uncertainties in the values found for K_D and E_0.

Next, we investigated the relative importance of the two sources of random errors, in pipetting and in counting. Fig. 7 *A* shows a spread of K_D and E_0 from 1000 virtual data sets simulated, where σ^i was set to 0.08 μL. Calculations including only the pipetting error are shown in Fig. 7 *B*. Calculations including only the counting error are shown in Fig. 7 *C*. These figures demonstrate that the pipetting error was the most important source of error in our experimental setup.

TABLE 2 The impact of different pipetting errors σ^i on the accuracy of the parameters K_D and E_0

σ^i (μL)	σK_D (%)	σE_0 (%)
0.00	5.6	1.2
0.04	6.6	2.1
0.08	9.4	3.5
0.12	12	5.1

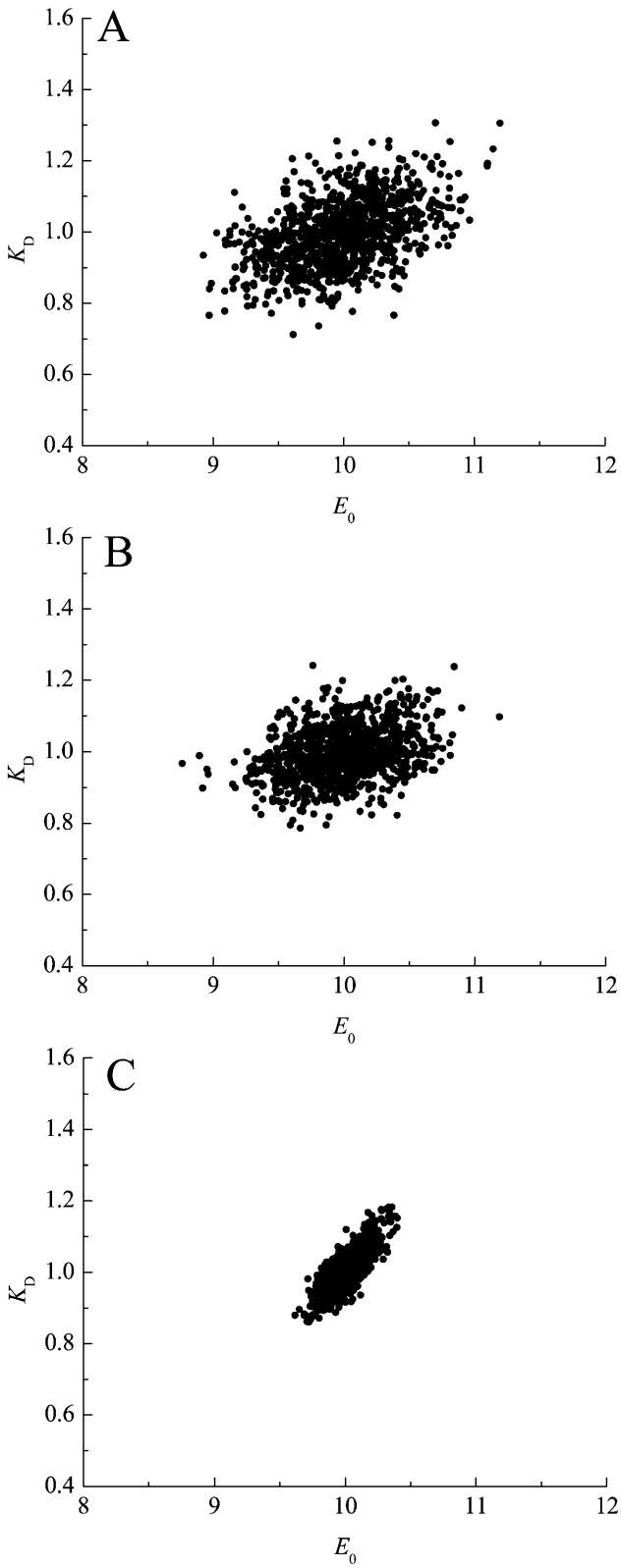

FIGURE 7 Effect of the value for the leak rate (*LR*) and β on the spread of the parameters K_D and E_0. (*A*) Spread of K_D and E_0 from 1000 virtual data sets, with σ^i set to 0.08 μL; σK_D (%) = 8.1, and σE_0 (%) = 3.5. (*B*) σ^i set to 0.08 μL, and β increased 1000 times; σK_D (%) = 7.2, and σE_0 (%) = 3.4. (*C*) σ^i set to 0.0 μL; σK_D (%) = 5.5, and σE_0 (%) = 1.2.

TABLE 3 The impact of the correction for different leak rates (*LR*) at different E_0/K_D ratios

	$LR = 0.0\%$/min*		$LR = 0.6\%$/min†		$LR = 1.2\%$/min‡	
E_0/K_D	K_D (σK_D in %)	E_0 (σE_0 in %)	K_D (σK_D in %)	E_0 (σE_0 in %)	K_D (σK_D in %)	E_0 (σE_0 in %)
1	1.4 (16)	1.3 (8)	1.0 (16)	1.0 (7)	0.7 (16)	0.7 (9)
3	1.2 (11)	3.4 (5)	1.0 (10)	3.0 (5)	0.8 (11)	2.6 (5)
10	1.2 (9)	10.9 (3)	1.0 (8)	10.0 (4)	0.8 (10)	9.3 (4)
30	1.2 (10)	31.6 (3)	1.0 (10)	30.1 (3)	0.9 (10)	28.6 (3)
100	1.2 (11)	104 (3)	1.0 (11)	100 (3)	0.8 (11)	96.4 (3)
300	1.3 (17)	311 (3)	1.0 (16)	299 (3)	0.8 (17)	220 (3)

*No leak correction.
†Correct leak rate.
‡Twice the correct leak rate.

For the high-affinity data set with wild-type EII^{mtl}, the standard deviations based on Monte Carlo simulations were 156 ± 6 nM for the K_D and 784 ± 14 nM for E_0. For the low-affinity data set on EII-G196D, these values were 25 ± 2 μM and 46 ± 1 μM.

Systematic errors

The effect of improper leak correction. To investigate the importance of leak correction (Eq. 5), we used the same Monte Carlo procedure to generate 200 virtual data sets under a range of conditions (E_0/K_D between 1 and 300), with *LR* equal to 0.6%/min. Analysis was done without leak correction ($LR = 0\%$/min) or with a two-times overestimated value ($LR = 1.2\%$ min). The results are shown in Table 3, with an example of the titration curve and scatter plot obtained at $E_0/K_D = 10$ (Fig. 8). The use of incorrect leak rates results in a similar systematic trend at all E_0/K_D ratios. In addition, it leads to larger uncertainties in the parameters K_D and E_0: up to 17% for the K_D, and 9% for E_0 (see Table 3).

The effect of an improper β-value. To investigate the importance of the parameter β, which relates the measured radioactivity with the concentration of free ligand in the upper compartment, we used the same Monte Carlo procedure. Virtual data sets, generated as described above with a given β-value, were analyzed with β-values equal to 0.95 or 1.05 times the value used for the simulations (the ''true'' value). An example of the titration curve and scatter plot obtained at $E_0/K_D = 10$ is shown in Fig. 9. Errors of this magnitude in β lead to significant errors in the binding parameters at E_0/K_D ratios <3 and >30. Moreover, the quality of the fits under these conditions was significantly worse, especially at the higher E_0/K_D ratios, where the χ^2 values were almost 50% higher (data not shown). This approach can be useful for recognizing such a systematic error. Under these conditions, one may decide to use β as the third parameter in a three-parameter fitting procedure, as will be discussed below.

The effect of improper weight factors. The importance of correct weight factors in Eq. 8 is illustrated by repeating the

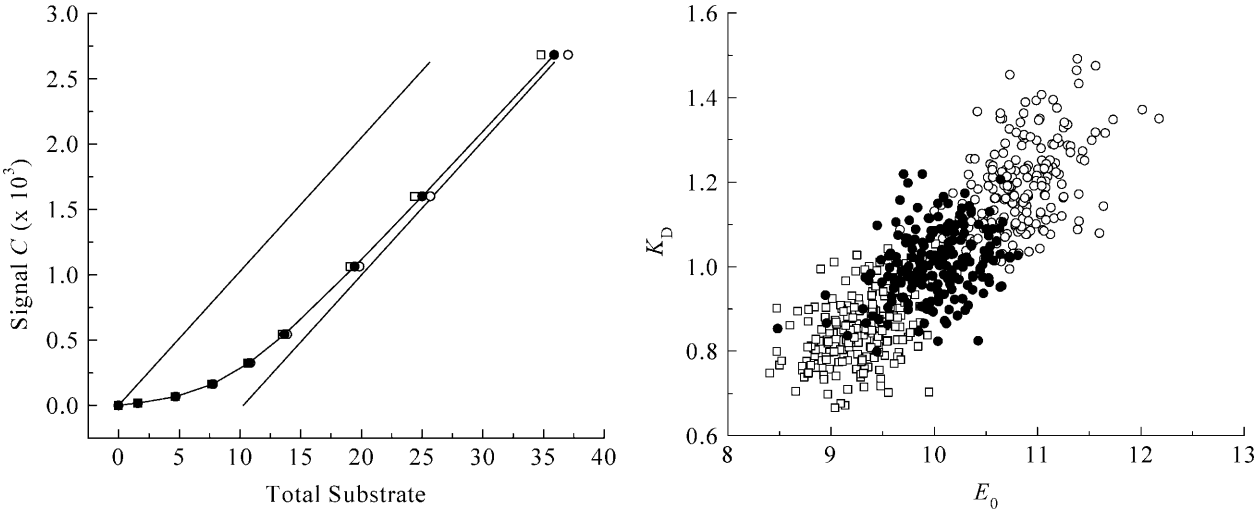

FIGURE 8 Effect of improper leak correction. Monte Carlo simulations and example titration curve at an E_0/K_D ratio of 10, with σ^i set to 0.08 μL. (○) $LR = 0.0\%$/min; σK_D (%) = 10.0, σE_0 (%) = 8.8. (●) $LR = 0.6\%$/min; σK_D (%) = 3.4, σE_0 (%) = 8.1. (□) $LR = 1.2\%$/min; σK_D (%) = 9.5, σE_0 (%) = 3.6.

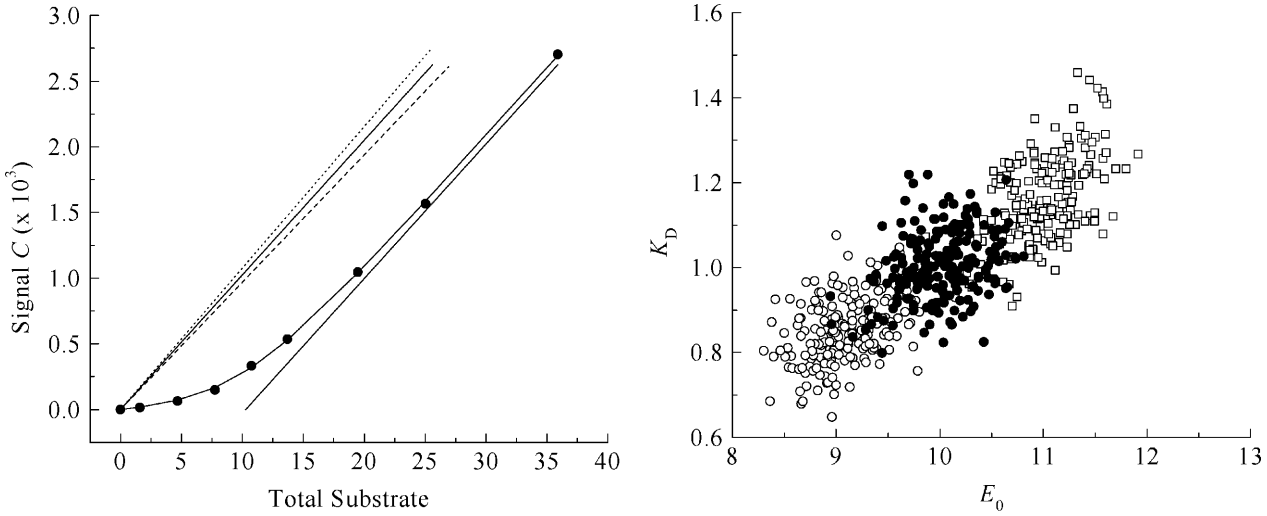

FIGURE 9 Effect of improper β-value. Monte Carlo simulations and example titration curve at an E_0/K_D ratio of 10, with σ^i set to 0.08 μL. Open circles and dashed line, $0.95 \times \beta$; σK_D (%) = 8.7, σE_0 (%) = 3.7; solid circles and solid line, $1.00 \times \beta$; σK_D (%) = 8.1, σE_0 (%) = 3.5; open squares and dotted line: $1.05 \times \beta$; σK_D (%) = 8.7, σE_0 (%) = 3.2.

above calculations and analyzing the resulting virtual data sets with equal weight factors for all data points. Neglecting the weight of the individual data points has a significant impact on the accuracy of the binding parameters, especially the K_D (see Table 4). The effect can be explained by noting that correct weight factors emphasize the first titration points relative to the last points, where pipetting errors have accumulated and the uncertainty in the calculated radioactivity counts has increased. Hence, the use of equal weight factors for all data points overrates the last titration points.

Three-parameter fit. The value for β in a flow dialysis experiment can in principle be extracted from the raw data, together with the K_D and E_0. We investigated this possibility to treat not only the binding parameters K_D and E_0 as fit parameters in our nonlinear least-squares regression procedure, but also the parameter β. Again we generated 1000 virtual data sets, and implemented a three-parameter fitting routine. Fig. 6 presents the obtained accuracy for K_D and E_0 at different E_0/K_D ratios (*open symbols*: *squares* for the K_D, *circles* for E_0). The optimal range for E_0 values is narrower than when two parameters are fitted (*solid symbols* in Fig. 6).

At E_0/K_D ratios <10, the spread in β was more than 7%, whereas at the higher E_0/K_D ratios, this spread was minimal (data not shown). We concluded that accurate results could only be obtained in the regime where saturation of the binding sites at the end of the titration was virtually complete and sufficient information for a proper estimation of β is present in the data. Interestingly, when incorrect leak rates were used for the analysis, the routine compensated for this systematic error by adjusting the value for β, such that the relevant binding parameters K_D and E_0 were still estimated correctly (data not shown).

TABLE 4 The impact of improper correction for the weights of the data points at different E_0/K_D ratios

E_0/K_D ratio	σK_D (%)	σE_0 (%)
1	16	8
3	13	5
10	13	4
30	20	4
100	37	3
300	71	3

DISCUSSION

The attractive features of flow dialysis to evaluate protein-ligand interactions, compared to other experimental approaches include i), the relatively short time needed to estimate K_D and E_0; ii), the simple setup/equipment that can be easily constructed in a workshop; and iii), the flexibility in detection mode, e.g., scintillation counting or optical spectroscopy, depending on the type of label used in the ligand. In principle, any binding event can be studied provided that the protein or other macromolecular species can be separated from the ligand by a semipermeable membrane.

Commonly, the standard deviations of the best-fit binding parameters are estimated from the curvature of the χ^2-function near its minimum. When only a small number of data points is available, these standard deviations can fluctuate significantly from one (virtual) binding experiment to the next, and the MC simulation procedure was found to be much more reliable. In addition, the MC simulations can be used to investigate where further improvements of the system can be worthwhile.

The differences in the leak rates observed in the high-affinity and low-affinity mannitol binding experiments is caused most likely by the use of two different batches of

semipermeable membranes. This further emphasizes the importance of the control experiments, since the value for LR (and hence β) can be dependent on the membrane batch used.

The three-parameter fitting procedure was initially built to see if it was possible to obtain all parameters (K_D, E_0, and β) within a single experiment. In this case, a control experiment would not be needed, provided the leak rate is known for a given experimental setup. Here we show that at low E_0/K_D ratios, the saturation level is too low to make a proper estimation of E_0 (see Fig. 6). The regime at which three parameters can be fitted properly with eight (averaged) data points is more restricted than when only two parameters must be fitted: for two-parameter fitting, the range is optimal at E_0/K_D ratios between 3 and 30, whereas for three-parameter fitting this range is narrowed down to E_0/K_D ratios between 10 and 30. Clearly, at the lower ratios the data points do not hold enough information to accurately determine β.

In conclusion, in this article a thorough evaluation of the accuracy of the flow-dialysis method is presented. Guidelines to optimize the experiment are given and the impact of all possible error sources that influence the K_D and E_0 parameters have been investigated. The use of these guidelines ensures an accurate and reliable measurement of both the K_D and E_0 in a single measurement.

This work was supported by the Netherlands Foundation for Chemical Research with financial aid from the Netherlands Organization for the Advancement of Scientific Research.

REFERENCES

André, I., and S. Linse. 2002. Measurements of Ca^{2+}-binding constants of proteins and presentation of the CaLigator software. *Anal. Biochem.* 305:195–205.

Boer, H., R. H. Ten Hoeve-Duurkens, J. S. Lolkema, and G. T. Robillard. 1995. Phosphorylation site mutants of the mannitol transport protein enzyme II^{mtl} of *Escherichia coli*: studies on the interaction between the mannitol translocating C-domain and the phosphorylation site on the energy coupling B-domain. *Biochemistry.* 34:3239–3247.

Broos, J., F. Ter Veld, and G. T. Robillard. 1999. Membrane protein-ligand interactions in *Escherichia coli* vesicles and living cells monitored via a biosynthetically incorporated tryptophan analogue. *Biochemistry.* 38:9798–9803.

Colowick, S. P., and F. C. Womack. 1969. Binding of diffusible molecules by macromolecules: rapid measurement by rate of dialysis. *J. Biol. Chem.* 244:774–777.

England, P., and G. Hervé. 1992. Synergistic inhibition of *Escherichia coli* aspartate transcarbamylase by CTP and UTP: binding studies using continuous-flow dialysis. *Biochemistry.* 31:9725–9732.

Feldmann, K. 1978. New devices for flow dialysis and ultrafiltration for the study of protein-ligand interactions. *Anal. Biochem.* 88:225–235.

Fuchs, H., and R. Gessner. 2001. The result of equilibrium-constant calculations strongly depends on the evaluation method used and on the type of experimental errors. *Biochem. J.* 359:411–418.

Hellingwerf, K. J., and W. N. Konings. 1980. Kinetic and steady-state investigations of solute accumulation in bacterial membranes by continuously monitoring the radioactivity in the effluent of flow-dialysis experiments. *Eur. J. Biochem.* 106:431–437.

Larsson, Å. 1997. Regression analysis if simulated radio-ligand equilibrium experiments using seven different mathematical models. *J. Immunol. Methods.* 206:135–142.

Lolkema, J. S., and G. T. Robillard. 1990. Subunit structure and activity of the mannitol-specific enzyme II of the *Escherichia coli* phosphoenolpyruvate-dependent phosphotransferase system solubilized in detergent. *Biochemistry.* 29:10120–10125.

Lolkema, J. S., D. Swaving-Dijkstra, and G. T. Robillard. 1992. Mechanics of solute translocation catalyzed by enzyme II^{mtl} of the phosphoenolpyruvate-dependent phosphotransferase system of *Escherichia coli*. *Biochemistry.* 31:5514–5521.

Lolkema, J. S., D. Swaving-Dijkstra, R. H. Ten Hoeve-Duurkens, and G. T. Robillard. 1990. The membrane-bound domain of the phosphotransferase enzyme II^{mtl} of *Escherichia coli* constitutes a mannitol translocation unit. *Biochemistry.* 29:10659–10663.

Lolkema, J. S., E. S. Wartna, and G. T. Robillard. 1993. Binding of the substrate analogue perseitol to phosphorylated and unphosphorylated enzyme II^{mtl} of the phosphoenolpyruvate-dependent phosphotransferase system of *Escherichia coli*. *Biochemistry.* 32:5848–5854.

Porumb, T. 1994. Determination of calcium-binding constants by flow dialysis. *Anal. Biochem.* 220:227–237.

Rovati, G. E., D. Rodbard, and P. J. Munson. 1988. DESIGN: computerized optimization of experimental design for estimating K_d and B_{max} in ligand binding experiments. *Anal. Biochem.* 174:636–649.

Schumacher, C., and V. von Tscharner. 1994. Practical instructions for radioactively labeled ligand receptor binding studies. *Anal. Biochem.* 222:262–269.

Westerhoff, H. V., A. H. C. A. Wiechmann, K. Van Dam, and K. J. Hellingwerf. 1989. On the evaluation of data from flow-dialysis experiments. *J. Biochem. Biophys. Methods.* 18:53–64.

Womack, F. C., and S. P. Colowick. 1973. Rapid measurement of binding of ligands by rate of dialysis. *Methods Enzymol.* 27:464–471.